

AD-A034 608 NAVAL RESEARCH LAB WASHINGTON D C
TRACKING FILTERS FOR MULTIPLE-PLATFORM RADAR INTEGRATION. (U)
DEC 76 G V TRUNK, J D WILSON

F/G 17/9

UNCLASSIFIED

NRL-8087

NL

1 OF 1
AD-A
034 608



END
DATE
FILMED
3-14-77
NTIS

U.S. DEPARTMENT OF COMMERCE
National Technical Information Service

AD-A034 608

TRACKING FILTERS FOR MULTIPLE-PLATFORM
RADAR INTEGRATION

NAVAL RESEARCH LABORATORY
WASHINGTON, D. C.

14 DECEMBER 1976

024107

NRL Report 8087

dc
ADA034608

Tracking Filters for Multiple-Platform Radar Integration

G. V. TRUNK AND J. D. WILSON

*Radar Analysis Staff
Radar Division*

December 14, 1976



REPRODUCED BY
**NATIONAL TECHNICAL
INFORMATION SERVICE**
U. S. DEPARTMENT OF COMMERCE
SPRINGFIELD, VA. 22161

NAVAL RESEARCH LABORATORY
Washington, D.C.

D D C
RECORDED
JAN 21 1977
D

Approved for public release; distribution unlimited.

SECURITY CLASSIFICATION OF THIS PAGE (When Data Entered)

REPORT DOCUMENTATION PAGE		READ INSTRUCTIONS BEFORE COMPLETING FORM
1. REPORT NUMBER NRL Report 8087	2. GOVT ACCESSION NO.	3. RECIPIENT'S CATALOG NUMBER
4. TITLE (and Subtitle) TRACKING FILTERS FOR MULTIPLE-PLATFORM RADAR INTEGRATION		5. TYPE OF REPORT & PERIOD COVERED Final Report on one phase of a continuing NRL problem
		6. PERFORMING ORG. REPORT NUMBER
7. AUTHOR(s) G. V. Trunk and J. D. Wilson		8. CONTRACT OR GRANT NUMBER(s)
9. PERFORMING ORGANIZATION NAME AND ADDRESS Naval Research Laboratory Washington, D.C. 20375		10. PROGRAM ELEMENT, PROJECT, TASK AREA & WORK UNIT NUMBERS NRL Problem R02-97 Program Element 61153N Project RR021-05-41
11. CONTROLLING OFFICE NAME AND ADDRESS Department of the Navy Office of Naval Research Arlington, Va. 22217		12. REPORT DATE December 14, 1976
		13. NUMBER OF PAGES 18
14. MONITORING AGENCY NAME & ADDRESS (if different from Controlling Office)		15. SECURITY CLASS. (of this report) UNCLASSIFIED 15a. DECLASSIFICATION/DOWNGRADING SCHEDULE
16. DISTRIBUTION STATEMENT (of this Report) Approved for public release; distribution unlimited		
17. DISTRIBUTION STATEMENT (of the abstract entered in Block 20, if different from Report)		
18. SUPPLEMENTARY NOTES		
19. KEY WORDS (Continue on reverse side if necessary and identify by block number) Tracking filters Multiple platforms α - β filters Least squares filter		
20. ABSTRACT (Continue on reverse side if necessary and identify by block number) The Kalman filter is the optimum tracking filter regardless of whether or not radar detections are made from single or multiple platforms. The performance of the Kalman filter has been simulated for various radar-target geometries. An error criterion involving the Mahalanobis distance function is used to detect target maneuvers, and an interactive scheme based on this criterion is used to increase the error covariance matrix to its proper value.		

(Continued)

DD FORM 1 JAN 73 1473

EDITION OF 1 NOV 65 IS OBSOLETE

S/N 0102-014-6601

SECURITY CLASSIFICATION OF THIS PAGE (When Data Entered)

20. Continued

Attempts to replace the Kalman filter with a simple filter with comparable performance have not been productive. The basic reason behind this difficulty is that accurate position and velocity estimates (obtainable by triangulation from different platforms) require the processing of position and velocity covariance matrices. Since both matrices must be saved and updated, a simple filter does not seem possible.

WHITE	White Section	<input checked="" type="checkbox"/>
WHITE	Buff Section	<input type="checkbox"/>
UNARMED		
ARMED		
VERIFICATION		
DT		
DISTRIBUTION/AVAILABILITY CODES		
DIST.	AVAIL. AND/OR SPECIAL	
A		

CONTENTS

INTRODUCTION	1
TRACKING FILTERS.....	1
Kalman Filter	2
Kalman Filter with a Turn Detector.....	6
Computational Requirements for the Kalman Filter	7
Modified Maximum-Likelihood Filter	7
Modified Maximum-Likelihood Filter with a Turn Detector. .	9
Computational Requirements for the Modified Maximum-Likelihood Filter	9
MONTE CARLO SIMULATION	10
Radar Geometry	10
Target Trajectory.....	10
Target Detection and Estimation	11
MONTE CARLO RESULTS	12
CONCLUSIONS	13
ACKNOWLEDGMENT	14
REFERENCES	15

D D C
 APPROVED
 JAN 21 1977
 RELEASED
 D

TRACKING FILTERS FOR MULTIPLE-PLATFORM RADAR INTEGRATION

INTRODUCTION

In the 1960's, fleet exercises demonstrated that many targets were not detected by radar operators. Furthermore postanalysis of video recordings of the radar data revealed that the radar return from the targets was present in the raw video. Some of the reasons operators missed targets were operator fatigue, collapsing of upper beams of the 3D radar onto a PPI display, jamming, and clutter. Therefore, to improve its surveillance capability, the Navy decided to associate automatic detection and tracking (ADT) systems with its radars. Specifically the SPS-48C and RVP (radar video processor) for 2D radars have been approved for fleet operation.

On board most naval combat vessels there are two kinds of surveillance radars: 2D radars (usually UHF band) and 3D radars (S band). In 1973 the Naval Research Laboratory [1-4] and the Applied Physics Laboratory (APL) of the Johns Hopkins University [5] embarked on programs to maximize the information aboard the vessel by integrating the radar data from different radars into a single track file. The benefits of such a system would be increased track life and on-line redundancy. At present the SYS-1-D system, an operational automatic detection and integrated tracking (ADIT) system developed by APL, is scheduled to be tested at sea in early 1977.

As an extension of the concept of integration more information can be obtained by combining the radar data from several platforms into a system track file. In addition to the advantages of an ADIT system, a platform-to-platform integration system will have inherent antijamming protection because of its frequency and spatial diversity. Some of the basic ideas and problems associated with such a system are discussed in NRL Memorandum Report 3404 [6]. In the current report some tracking filters that can be used for platform-to-platform tracking are discussed.

The basic tracking philosophy and two tracking algorithms (Kalman filter and an uncoupled maximum-likelihood filter) are discussed in the next section. The accuracy of the two filters is compared by using a Monte Carlo simulation. The simulation is discussed in the third section, and the results are given in the fourth section. The conclusions are made in the fifth section.

TRACKING FILTERS

Since the raw detections contain the maximum amount of information, communication bandwidth restrictions will be ignored, and it will be assumed that *all* detections will be used to update a track. All detections do not contain the same amount of information [6]: one radar could be more accurate than another, or a second detection could

TRUNK AND WILSON

immediately follow (in time) a previous detection. Consequently what is required is a method of filtering the data (before transmission over the communication channel) to obtain the detections containing the most information. Then only these detections would be used to update the track. However, since the question of filtering the detections is still open, it is assumed in this report that all detections are used to update the track.

The first filter considered is the Kalman filter in xy coordinates. Since the storage and computation requirements are somewhat large, an uncoupled maximum-likelihood filter is also considered.

Kalman Filter

The Kalman filter is a recursive filter which minimizes the least-square error. The state equation in xy coordinates [7], which in our case represents the equation of motion, is

$$X(t+1) = \Phi(t)X(t) + \Gamma(t)A(t), \quad (1)$$

$$\text{where } X(t) = \begin{bmatrix} x(t) \\ \dot{x}(t) \\ y(t) \\ \dot{y}(t) \end{bmatrix}, \quad \Phi(t) = \begin{bmatrix} 1 & T & 0 & 0 \\ 0 & 1 & 0 & 0 \\ 0 & 0 & 1 & T \\ 0 & 0 & 0 & 1 \end{bmatrix}, \quad \Gamma(t) = \begin{bmatrix} \frac{1}{2}T^2 & 0 \\ T & 0 \\ 0 & \frac{1}{2}T^2 \\ 0 & T \end{bmatrix}, \text{ and } A(t) = \begin{bmatrix} a_x(t) \\ a_y(t) \end{bmatrix},$$

with $X(t)$ being the state vector at time t consisting of position and velocity components $x(t)$, $\dot{x}(t)$, $y(t)$, and $\dot{y}(t)$, $t+1$ being the next observation time, T being the time between observations, and $a_x(t)$ and $a_y(t)$ being random accelerations whose covariance matrix is $Q(t)$. The observation equation is

$$Y(t) = M(t)X(t) + V(t), \quad (2)$$

$$\text{where } Y(t) = \begin{bmatrix} x_m(t) \\ y_m(t) \end{bmatrix}, \quad M(t) = \begin{bmatrix} 1 & 0 & 0 & 0 \\ 0 & 0 & 1 & 0 \end{bmatrix}, \text{ and } V(t) = \begin{bmatrix} v_x(t) \\ v_y(t) \end{bmatrix},$$

with $Y(t)$ being the measurement at time t consisting of positions $x_m(t)$ and $y_m(t)$ and $V(t)$ being zero mean noise whose covariance matrix is $R(t)$.

The problem is solved recursively by first assuming the problem is solved at time $t-1$. Specifically it is assumed that the best estimate $\hat{X}(t-1|t-1)$ at time $t-1$ and its error covariance matrix $P(t-1|t-1)$ are known, where the circumflex signifies an estimate and $\hat{X}(t|s)$ signifies that $X(t)$ is being estimated with observations up to $Y(s)$. The six steps involved in the recursive algorithm are as follows:

Step 1. Calculate one step prediction,

$$\hat{X}(t|t-1) = \Phi(t-1) \hat{X}(t-1|t-1); \quad (3)$$

Step 2. Calculate the covariance matrix for one step prediction,

$$P(t|t-1) = \Phi(t-1) P(t-1|t-1) \tilde{\Phi}(t-1) + \Gamma(t-1) Q(t-1) \tilde{\Gamma}(t-1); \quad (4)$$

Step 3. Calculate the prediction observation,

$$\hat{Y}(t|t-1) = M(t) \hat{X}(t|t-1); \quad (5)$$

Step 4. Calculate the filter gain,

$$\Delta(t) = P(t|t-1) \tilde{M}(t) [M(t) P(t|t-1) \tilde{M}(t) + R(t)]^{-1}; \quad (6)$$

Step 5. Calculate a new smoothed estimate,

$$\hat{X}(t|t) = \hat{X}(t|t-1) + \Delta(t) [Y(t) - \hat{Y}(t|t-1)]; \quad (7)$$

Step 6. Calculate a new covariance matrix,

$$P(t|t) = [I - \Delta(t) M(t)] P(t|t-1). \quad (8)$$

In summary, starting with an estimate $\hat{X}(t-1|t-1)$ and its covariance matrix $P(t-1|t-1)$, after receiving a new observation $Y(t)$ and calculating the six quantities in the recursive algorithm, a new estimate $\hat{X}(t|t)$ and its covariance matrix $P(t|t)$ are obtained.

For the Kalman filter in xy coordinates, the measurement covariance matrix $R(t)$ is a function of the radar-target geometry. Letting (at time t) r_t and θ_t be the range and azimuth of the target with respect to the radar (with the azimuth angle being measured counterclockwise from the x axis), the elements of the covariance matrix

$$R(t) = \begin{vmatrix} \sigma_x^2(t) & \sigma_{xy}^2(t) \\ \sigma_{xy}^2(t) & \sigma_y^2(t) \end{vmatrix}, \quad (9)$$

are

$$\sigma_x^2(t) = \sigma_r^2 \cos^2 \theta_t + r_t^2 \sigma_\theta^2 \sin^2 \theta_t, \quad (10)$$

$$\sigma_y^2(t) = \sigma_r^2 \sin^2 \theta_t + r_t^2 \sigma_\theta^2 \cos^2 \theta_t, \quad (11)$$

and

$$\sigma_{xy}^2(t) = [\sigma_r^2 - r_t^2 \sigma_\theta^2] \sin \theta_t \cos \theta_t, \quad (12)$$

where σ_r^2 and σ_θ^2 are the variances of the range and azimuth measurement errors respectively.

TRUNK AND WILSON

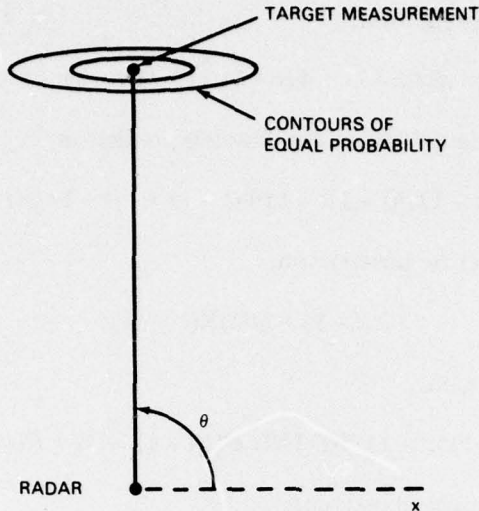


Fig. 1 — Typical contours of equal probability for the position of a target that is detected

For the assumption that the measurement errors are Gaussian, typical contours of equal probability are shown in Fig. 1. If $\sigma_r = 100 \text{ m}$, $\sigma_\theta = 0.3^\circ$, $r = 2 \times 10^5 \text{ m}$, and $\theta = 90^\circ$, the corresponding covariance matrix is

$$R \approx \begin{bmatrix} 10^6 & 0 \\ 0 & 10^4 \end{bmatrix}. \quad (13)$$

Thus the radar measures the y coordinate, corresponding to range, rather accurately and the x coordinate, corresponding to azimuth, rather inaccurately. If a Kalman filter is used for the radar geometry shown in Fig. 1, the covariance matrix $P(t|t)$ will be of the form

$$P(t|t) = \begin{bmatrix} H(t) & 0 \\ 0 & L(t) \end{bmatrix}, \quad (14)$$

where $H(t)$ and $L(t)$ are two-by-two matrices and the terms in H are approximately 100 times greater than the corresponding terms in L . The filter gain $\Delta(t)$ is of the form

$$\Delta(t) = \begin{bmatrix} \alpha_x(t) & 0 \\ \beta_x(t) & 0 \\ 0 & \alpha_y(t) \\ 0 & \beta_y(t) \end{bmatrix}, \quad (15)$$

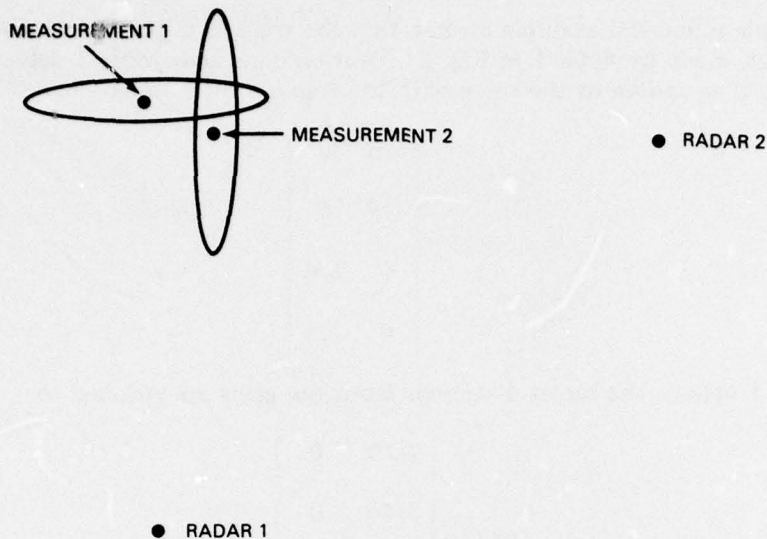


Fig. 2 — Geometry of two radars and of where they detect a target

and furthermore $\alpha_x(t) \approx \alpha_y(t)$ and $\beta_x(t) \approx \beta_y(t)$. The filter gains would be identical if the target's range change were only a fraction of its initial range (the x -measurement variance $r^2 \sigma_\theta^2$ must remain relatively constant).

If at some instant in time a second radar with a different aspect angle detects the target, the situation changes significantly. For example, if as shown in Fig. 2 a second radar detects the target at an azimuth of 180° at the same range with the same accuracy as the first radar, its measurement covariance is of the form

$$R(t+1) = \begin{bmatrix} 10^4 & 0 \\ 0 & 10^6 \end{bmatrix}. \quad (16)$$

The filter gain $\Delta(t+1)$ is of the form

$$\Delta(t+1) = \begin{bmatrix} \alpha_x(t+1) & 0 \\ \beta_x(t+1) & 0 \\ 0 & \alpha_y(t+1) \\ 0 & \beta_y(t+1) \end{bmatrix}, \quad (17)$$

and $\alpha_x(t+1) \approx 1$, $\beta_x(t+1) > \beta_x(t)$, $\alpha_y(t+1) \approx 0$, and $\beta_y(t+1) \approx 0$. That is, initially radar 1 was providing an accurate y measurement and an inaccurate x measurement. When radar 2 provided an accurate x measurement and an inaccurate y measurement, the accurate measurement is given a weighting of 1, and the inaccurate measurement is given a weighting of 0.

TRUNK AND WILSON

As a simple numerical example assume that the track is initiated by two detections, 4 seconds apart, made by radar 1 in Fig. 2. Four seconds later radar 1 detects the target and makes the first update of the track with the Kalman filter gains

$$\Delta(1) = \begin{vmatrix} 5/6 & 0 \\ 1/8 & 0 \\ 0 & 5/6 \\ 0 & 1/8 \end{vmatrix}. \quad (18)$$

If again radar 1 detects the target 4 seconds later, the gains are reduced to

$$\Delta(2) = \begin{vmatrix} 7/10 & 0 \\ 3/40 & 0 \\ 0 & 7/10 \\ 0 & 3/40 \end{vmatrix}. \quad (19)$$

However, if radar 2 makes the next detection 4 seconds later, the gains are

$$\Delta(3) = \begin{vmatrix} 1 & 0 \\ 1/12 & 0 \\ 0 & 10^{-2} \\ 0 & 10^{-3} \end{vmatrix}. \quad (20)$$

The gain for the x velocity rose only to $1/12$ because the old x measurement, which is used to calculate the x velocity, is rather inaccurate. However, when a second detection from radar 2 is made, $\beta_x(\cdot)$ will rise considerably, since an accurate x velocity can now be estimated.

Kalman Filter with a Turn Detector

The Kalman filter is the optimum filter as long as the target trajectory obeys the state equation (1), which describes a straight-line trajectory with random perturbations (the random perturbations bound the filter gains away from zero). However, when the target maneuvers, the maneuver must be detected and the error covariance matrix must be increased. In this study the error criterion is

$$\begin{aligned} E = & [\hat{X}(t|t-1) - \hat{X}(t|t)] \hat{M} [M P(t|t-1) \hat{M}]^{-1} M [\hat{X}(t|t-1) - \hat{X}(t|t)] \\ & + [Y(t) - M \hat{X}(t|t)] R(t)^{-1} [Y(t) - M \hat{X}(t|t)]. \end{aligned} \quad (21)$$

This error is the squared Mahalanobis distance from the smooth position $\hat{M}\hat{X}(t|t)$ to the predicted position $\hat{M}\hat{X}(t|t-1)$ plus the squared Mahalanobis distance from the smooth position $\hat{M}\hat{X}(t|t)$ to the measured position $Y(t)$. The Mahalanobis distance differs from the Euclidean distance by using a covariance-matrix kernel instead of an identity matrix.

When the error E is greater than a threshold (which in this study was set to $E = 16$, corresponding for example to covariance matrices that are diagonal and smooth coordinates that differ from the predicted and measured positions by twice the standard deviation), the error covariance matrix $P(t-1|t-1)$ is increased and a new smooth position $\hat{M}\hat{X}(t|t)$ is calculated. Increasing $P(t-1|t-1)$ causes the new position estimate $M\hat{X}(t|t)$ to be closer to the measurement $Y(t)$ and further from the prediction $\hat{X}(t|t-1)$. Since $P(t|t-1)$ increases when $P(t-1|t-1)$ increased, this increase in $P(t-1|t-1)$ will always cause E to decrease. This procedure is repeated until E is less than the threshold. Specifically terms P_{11} , P_{13} , P_{31} , and P_{33} are increased by \sqrt{F} ; terms P_{12} , P_{14} , P_{21} , P_{23} , P_{32} , P_{34} , P_{40} , and P_{43} are increased by F ; and terms P_{22} , P_{24} , P_{42} , and P_{44} are increased by F^2 . (In this study $F = 1.5^n$, where n is the number of consecutive covariance matrix increases.) The position covariance elements are not increased as much as the velocity elements because of coupling; that is, an uncertainty in predicted position is due not only to the uncertainty in the last position but also in the velocity. In a real system the track should also be bifurcated when a large error is encountered.

Computational Requirements for the Kalman Filter

Since the computational load in performing the Kalman filter (equations (3) through (8)) appears formidable, care was taken to minimize the number of calculations (additions and multiplications). The Kalman filter requires 50 additions and 61 multiplications. These numbers take into account the symmetry of covariance matrices and the simplicity of certain matrices; for example, $HP(t|t-1)\hat{H}$ removes four elements from a four-by-four matrix and consequently requires no additions or multiplications.

The storage requirement of the Kalman filter, in addition to the positions and velocities, is the ten unique elements of the covariance matrix. In an effort to reduce the computational load and the storage requirements, a modified maximum-likelihood approach was used.

Modified Maximum-Likelihood Filter

In this subsection, it will be assumed that the predicted and measured variables are independent and Gaussian. If the position and velocity variables were considered jointly, the maximum-likelihood method would yield the Kalman filter. Consequently, to reduce the complexity, position and velocity are considered separately.

The joint density of the predicted position X_p and measured position X_m is

$$P(X_p, X_m) = \left[\frac{1}{\sqrt{|2\pi K_p|}} e^{-(1/2)(\widetilde{x_p - \mu}) K_p^{-1} (x_p - \mu)} \right] \left[\frac{1}{\sqrt{|2\pi K_m|}} e^{-(1/2)(\widetilde{x_m - \mu}) K_m^{-1} (x_m - \mu)} \right], \quad (22)$$

TRUNK AND WILSON

where K_p and K_m are the predicted-position and measured-position covariance matrices respectively. The maximum-likelihood estimate of the position μ is that value of μ which maximizes (22). Taking the partial derivative of the log of (22) with respect to μ yields the expression

$$K_p^{-1}(X_p - \mu) + K_m^{-1}(X_m - \mu). \quad (23)$$

When (23) is set equal to 0 and solved for μ , the maximum-likelihood estimate is obtained as

$$\hat{\mu} = (K_p^{-1} + K_m^{-1})^{-1} (K_p^{-1}X_p + K_m^{-1}X_m). \quad (24)$$

It is straightforward to show that the covariance of $\hat{\mu}$ is

$$K_\mu = E\{\hat{\mu} \hat{\mu}^\top\} = (K_m^{-1} + K_p^{-1})^{-1}. \quad (25)$$

Using the new position estimate $\hat{\mu}$ and the old smoothed position, a new velocity estimate can be obtained. Then the new velocity estimate can be combined with old velocity estimate using an equation with the identical form of (24).

In summary, the problem is originally solved for a given instant in time. Specifically the smoothed position X_s and smoothed velocity V_s and their corresponding covariance matrices K_x and K_v^{-1} (inverse) are available. After T seconds a new position X_m is measured; and the new estimates and covariances are found by calculating the eight quantities in the following algorithm:

Step 1. Calculate the predicted position X_p ,

$$X_p = X_s + V_s T; \quad (26)$$

Step 2. Calculate the covariance matrix (assuming X_s and V_s are independent) for prediction,

$$K_p = K_x + T^2 K_v; \quad (27)$$

Step 3. Calculate the covariance matrix for the smoothed position estimate,

$$K_\mu = (K_p^{-1} + K_m^{-1})^{-1}; \quad (28)$$

Step 4. Calculate the smoothed position estimate,

$$\hat{\mu} = K_\mu (K_p^{-1} X_p + K_m^{-1} X_m); \quad (29)$$

Step 5. Calculate the new velocity estimate,

$$V_N = (\hat{\mu} - X_s)/T; \quad (30)$$

Step 6. Calculate the covariance matrix (assuming μ and X_s are independent) for the new velocity estimate,

$$K_N = (K_\mu + K_X)/T^2; \quad (31)$$

Step 7. Calculate the inverse covariance matrix for the smoothed velocity estimate,

$$K_{\hat{v}}^{-1} = (K_v^{-1} + K_N^{-1}); \quad (32)$$

Step 8. Calculate the smoothed velocity estimate,

$$\hat{V} = K_{\hat{v}} (K_v^{-1} V_s + K_N^{-1} V_N). \quad (33)$$

These eight steps complete the cycle: (29) is the smoothed position estimate, (28) is its covariance matrix, (33) is the smoothed velocity estimate, and (32) is its covariance matrix.

Modified Maximum-Likelihood Filter with a Turn Detector

The turn detector is the same one which was used for the Kalman filter. In terms of the new parameters the error criterion is

$$E = (\widetilde{X_p - \mu}) K_p^{-1} (\widetilde{X_p - \mu}) + (\widetilde{X_m - \mu}) K_m^{-1} (\widetilde{X_m - \mu}). \quad (34)$$

When the error exceeds 16, the covariance matrices K_s and K_v are both increased by the factor F (presently $F = 1.25$). The covariance matrices are continually increased by F until $E \leq 16$. Although there is no reason for increasing K_s and K_v by the same factor, this procedure has led to good results.

Computational Requirements For the Modified Maximum-Likelihood Filter

Taking into account the symmetry of the covariance matrices, the maximum-likelihood method (equations (26) through (33)) requires 37 additions and 59 multiplications. The storage requirements, in addition to the positions and velocities, are the six unique covariance elements of the two covariance matrices K_s and K_v . Comparing these results with those of the Kalman filter, it is seen that the maximum-likelihood method provides little computational advantage. This is because the calculations are essentially repeated twice for the maximum-likelihood method: once for the smooth position and once for the smooth velocity. All attempts to simplify the filter by using only one covariance matrix have failed. The reason is demonstrated by the example's gains given in (18), (19), and (20). In the example, when the system receives its first measurement from radar 2, the position gain is set close to 1. However it is not until the second measurement from radar 2 that the velocity gain will rise significantly. Since there may be a considerable time delay in obtaining this second measurement, two covariance matrices must be saved. The need to save two covariance matrices, with the cross terms supplying the crucial information for triangulation of a target, has aborted all attempts to simplify the tracking filter.

MONTE CARLO SIMULATION

Since the performance of the tracking filters during target maneuvers is extremely difficult to calculate analytically, a Monte Carlo simulation was used.

Radar Geometry

The simulation involves two platforms. The first ship is centered at the origin of an xy coordinate system ($x_1 = y_1 = 0$) whose x axis is through the bow of the ship. The second ship is at coordinates (x_2, y_2) and is oriented parallel to the first ship. Azimuth is measured as usual in an xy coordinate system: target at (x, y) with respect to radar i has azimuth angle $\theta_i = \tan^{-1}[(y - y_i)/(x - x_i)]$. The rolling and pitching of the ships are assumed to be periodic and are given by

$$R_i(t) = R_M \sin \left(\frac{2\pi t}{T_R} + \gamma_i \right) \quad (35)$$

and

$$P_i(t) = P_M \sin \left(\frac{2\pi t}{T_P} + \xi_i \right), \quad (36)$$

where R_M and P_M are the maximum roll and pitch angles, T_R and T_P are the roll and pitch periods, which are independent and uniformly distributed between 10 and 12 seconds, and γ_i and ξ_i are independent phase angles uniformly distributed on 0 to 2π .

Target Trajectory

The target flight profile is specified by an initial range, altitude, azimuth, speed, and heading. The target proceeds along this heading until time t_s , when the target starts a counterclockwise turn at a specified g value. At t_e the target ends the turn and proceeds along a straight line at its present heading. The elevation angle of the target is calculated by letting x , y , and z be the target coordinates on a flat earth and x_i , y_i , and h_r be the radar coordinates. Then, if the $4/3$ radius of the earth is denoted by R_e and if the notation

$$R_g = [(x - x_i)^2 + (y - y_i)^2]^{1/2} \quad (37)$$

and

$$B = \left(0.5 \frac{R_g}{R_e} \right)^{1/2} - \left(\frac{h_r}{R_g} \right)^{1/2} \quad (38)$$

is introduced, then the elevation angle e of the target is given [8] by

$$e = \tan^{-1} \left(\frac{Z}{R_g} - B^2 \right). \quad (39)$$

Target Detection and Estimation

The scan time for radar 1 is uniformly distributed between 3.9 and 4.1 seconds, and the scan time for radar 2 is uniformly distributed between 4.9 and 5.1 seconds. The initial time radar 1 passes over the target is $t = 0$, and the initial time radar 2 sweeps past the target is uniformly distributed between zero and the scan time of radar 2.

The question of whether or not a target is detected is resolved by first calculating the target signal-to-noise ratio (S/N). Using Blake's model [9], the multipath propagation factor F is calculated. Then the S/N is calculated using

$$S/N = 20\sigma_T \left(\frac{F R_D}{R} \right)^4, \quad (40)$$

where σ_T is the target cross section in square meters, R_D is the range where the probability of detection P_D is 0.9 and the probability of false alarm P_{fa} is 10^{-6} for a 1-square-meter target, and R is the target range. Using curves from Robertson [10], one obtains the P_D at $P_{fa} = 10^{-6}$ for the calculated S/N. A uniformly distributed random number between 0 and 1 is generated, and if the number is below P_D , the target is declared to be detected.

If the antenna is unstabilized and if a_i and e_i are the true azimuth and elevation angles of the target, the measured angles are [11]

$$a_m(i) = \tan^{-1} \left[\frac{\sin a_i \cos R_i + (\cos a_i \sin P_i + \tan e_i \cos P_i) \sin R_i}{\cos a_i \cos P_i - \tan e_i \sin P_i} \right] + \epsilon_{i1} \quad (41)$$

and

$$e_m(i) = \sin^{-1} [\cos e_i \cos a_i \sin P_i + \sin e_i \cos P_i] \cos R_i - \cos e_i \sin a_i \sin R_i + \epsilon_{i2}, \quad (42)$$

where ϵ_{i1} and ϵ_{i2} are independent Gaussian random variables with variances σ_a^2 and σ_r^2 respectively. Letting U and V be independent uniformly distributed random variables between 0 and 1, Gaussian variables with mean zero and variance σ^2 can be generated by

$$\epsilon = \sigma(-2 \log U)^{1/2} \cos(2\pi V). \quad (43)$$

If one measured only $a_m(i)$ and not $e_m(i)$, one would have large azimuth errors. For instance, if $R_m = 10^\circ$, $P_m = 5^\circ$, and $e = 15^\circ$, the azimuth error can be as large as 5° even though $\sigma_a = 0.5^\circ$ [12]. However, if $e_m(i)$ is measured and R_i and P_i are known, the measurements $a_m(i)$ and $e_m(i)$ which are relative to the deck plane of the ship can be rotated into a system whose xy plane is the plane of the ocean. These equations, which were derived by George as cited in Ref. 13, are

$$a'_m(i) = \tan^{-1} \left[\frac{-\sin R_i \sin e_m(i) + \cos R_i \sin a_m(i) \cos e_m(i)}{\cos P_i \cos a_m(i) \cos e_m(i) + W \sin P_i} \right] \quad (44)$$

TRUNK AND WILSON

$$e'_m(i) = \sin^{-1} [\sin P_i \cos a_m(i) \cos e_m(i) + W \cos P_i], \quad (45)$$

where

$$W = \cos R_i \sin e_m(i) + \sin R_i \sin a_m(i) \cos e_m(i).$$

Radars involved in platform-to-platform radar integration need elevation information [6] to transmit useful information from one platform to another. Thus, elevation angles are available to perform the appropriate corrections.

MONTE CARLO RESULTS

In this section results of the Kalman and maximum-likelihood filters are obtained for the radar geometry and target trajectories shown in Fig. 3. The radar coordinates are (0, 0) and (60, -60) km and the radar heights are 23 m. The target-trajectory parameters are given in Table 1.

It will be assumed that both radars have the same accuracies. Specifically the standard deviations of the range, azimuth, and elevation measurements are $\sigma_r = 150$ m, $\sigma_a = 0.3^\circ$, and $\sigma_e = 0.3^\circ$.

The performance measure for the tracking filter will be a modified RMS velocity error defined by

$$V_{\text{RMS}} = \left(\frac{1}{N} \sum_{i=1}^N \{ [\hat{V}_x(i) - V_x(i)]^2 + [\hat{V}_y(i) - V_y(i)]^2 \} \right)^{1/2}, \quad (46)$$

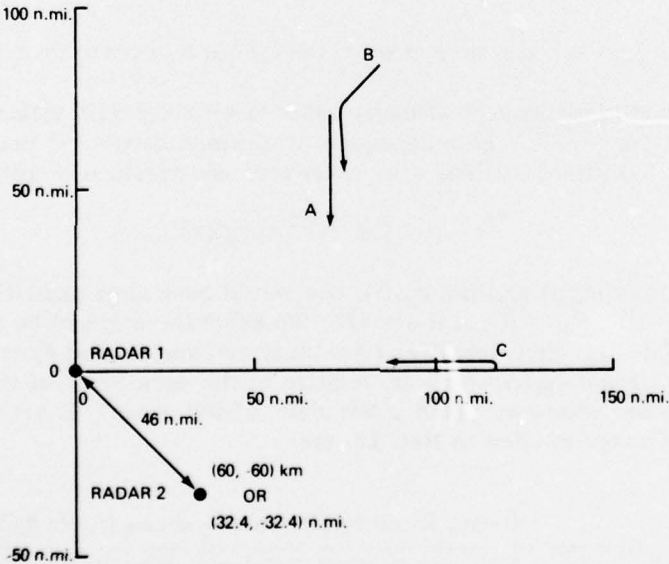


Fig. 3 — Geometry of two radars involved in platform-to-platform radar integration and of three cases of target trajectories

Table 1 — Target Trajectory Parameters (shown in Fig. 3)

Case	Range (n.mi.)	Azimuth (deg)	Heading (deg)	Speed (m/s)	Altitude (m)	Cross Section (m ²)	Target Maneuver			Roll R_M (deg)	Pitch P_M (deg)
							Start (s)	End (s)	Turn (g's)		
A	100	45	-90	300	15000	0.5	300	300	3	15	5
B	120	45	-135	300	4500	0.5	100	111.0	3	15	5
C	100	0	0	300	4500	1.0	100	132.7	3	15	5

where $V_x(i)$ and $V_y(i)$ are the true velocities, $\hat{V}_x(i)$ and $\hat{V}_y(i)$ are the estimated velocities, and the asterisk indicates that the sum excludes points between t_s and $t_e + 10$. The samples at the turn are excluded because during a turn the errors are large and would dominate V_{RMS} . During a turn what is important is the ability to detect the turn. Since both filters have the same turn detector (comparison of (21) to 16), the filters will have the same performance in this area. In the simulation the radar platforms are assumed to be gridlocked.

The simulation was run five times for the two filters and three target trajectories, and the average V_{RMS} is given in Table 2. As one would expect, the Kalman filter provides the more accurate track. Comparison of case-by-case results show that the Kalman filter reacts more rapidly when a poor initial estimate is made. For example, the velocity estimates for the third run of case B are shown in Table 3. The initial velocities are the same, the initialization algorithm being the same. As can be seen from Table 3, while the velocities from both filters are approaching the true values ($V_x = V_y = -215$ m/s), the velocity from the Kalman filter is approaching more rapidly.

Probably adjustments could be made to quicken the convergence of the maximum-likelihood algorithm. However, since the maximum-likelihood filter is almost as complicated as the Kalman filter, no changes were made, because the Kalman filter would be used rather than the maximum-likelihood filter.

CONCLUSIONS

The Kalman filter is the optimum tracking filter (with respect to the mean-square error) regardless of whether or not the radar detections are made from single or multiple platforms. The performance (specifically the RMS velocity error) of the Kalman filter for two platforms, separated by 46 n.mi., has been calculated for various target trajectories. An error criterion involving the squared Mahalanobis distances between the smooth and predicted positions and the smooth and measured positions is used to detect target maneuvers. After a turn has been detected, the covariance matrix is increased (in steps) until the error criterion is below a critical value.

Attempts to find a simple filter, with good performance, have not been productive. The maximum-likelihood filter obtained by arbitrarily decoupling the position and velocity estimates, although obtaining acceptable performance, is almost as complicated as

TRUNK AND WILSON

**Table 2 — Average V_{RMS} (Eq. (46))
For Five Runs of Each of the Cases
in Fig. 3**

Case	Average V_{RMS} (m/s)	
	Kalman Filter	Maximum-Likelihood Filter
A	16	23
B	32	60
C	22	32

**Table 3 — Velocity Estimates During the
Third Run of Case B**

Time	Velocity Estimates (m/s)			
	Kalman Filter		Maximum-Likelihood Filter	
	V_X	V_Y	V_X	V_Y
12.1	23	-451	23	-451
16.2	-125	-310	-30	-400
20.2	-154	-274	-57	-370
24.3	-174	-248	-82	-341
27.4	-162	-261	-105	-316
28.3	-161	-264	-104	-317
32.4	-164	-258	-118	-301
32.4	-170	-251	-118	-301
36.4	-189	-232	-146	-272

the Kalman filter and consequently would not be used. The basic reason behind this difficulty is that accurate position and velocity estimates (obtained by triangulation) require the processing of position and velocity covariance matrices. Since both matrices must be saved and updated, a simple filter does not seem possible.

In summary, the Kalman filter with a turn detector should be used as the tracking filter for radar detections from multiple platforms.

ACKNOWLEDGMENT

We thank Dr. B. H. Cantrell for various discussions about the tracking problem.

REFERENCES

1. G.V. Trunk, B.H. Cantrell, and F.D. Queen, "Basic System Concept for Integrating a 2D and a 3D Radar and Designs of Automatic Detection Systems," NRL Report 7678, Mar. 7, 1974.
2. B.H. Cantrell, G.V. Trunk, and J.D. Wilson, "Tracking System for Two Asynchronously Scanning Radars," NRL Report 7841, Dec. 5, 1974.
3. B.H. Cantrell, G.V. Trunk, F.D. Queen, J.D. Wilson, and J.J. Alter, "Automatic Detection and Integrated Tracking System," International Radar Conference Record, pp. 391-395, Apr. 1975.
4. J.D. Wilson and B.H. Cantrell, "Tracking System for Asynchronously Scanning Radars with New Correlation Techniques and an Adaptive Filter," NRL Report 7952, Jan. 4, 1976.
5. "Program Performance Specification for an AN-SYS-1 Detector/Trackor Sub-System of the DDG 2-15 Combat Weapon System," Applied Physics Lab, Johns Hopkins University, XWS-15612, Aug. 1975.
6. B.H. Cantrell, A. Grindlay, and C.H. Dodge, "Formulation of a Platform-to-Platform Radar Integration System," NRL Memorandum Report 3404, Dec. 1976.
7. F.R. Castella and F.G. Dunnebacke, "Analytical Results for the x, y Kalman Tracking Filter," *IEEE Trans on Aerospace and Electronic Systems AES-10* (No. 6) 891-895 (Nov. 1974).
8. D.J. Kaplan, A. Grindlay, and L. Davis, "Surveillance Radar Systems Evaluation Model (SURSEM) Handbook," NRL Report 8037, Dec. 23, 1976.
9. L.V. Blake, "Machine Plotting of Radio/Radar Vertical-Plane Coverage Diagrams, NRL Report 7098, June 1970.
10. G.H. Robertson, "Operating Characteristic for a Linear Detector of CW Signals in Narrow-Band Gaussian Noise," *Bell Sys. Tech J.* 46, 755-774 (1967).
11. W.M. Cady et al., editors, *Radar Scanners and Radomes*, Vol. 26, Radiation Laboratory Series, MIT, New York, McGraw-Hill, 1948.
12. G.V. Trunk, "Tracking Accuracy of the Mirror Scan Antenna in a 2D Configuration," NRL Report 7982, Apr. 1976.
13. B.H. Cantrell and G.V. Trunk, "Analysis of the Track Handoff Between the Search and Track Radars," NRL Report 7505, Dec. 29, 1972, p. 6.